Analogues of Natural Macarangin B Display Potent Antiviral Activity and Better Metabolic Stability

Gwenaëlle Jézéquel, Jules Fargier, Joëlle Bigay, Joël Polidori, Justine Geslin, Nathalie Hue, Chaker El Kalamouni, Sandy Desrat, Fanny Roussi

Analogues of Natural Macarangin B Display Potent Antiviral Activity and Better Metabolic Stability

Gwenaëlle Jézéquel,[a] Jules Fargier,[a] Joëlle Bigay,[b] Joël Polidori,[b] Justine Geslin,[c] Nathalie Hue,[a] Chaker El Kalamouni,[c] Sandy Desrat,[a] and Fanny Roussi*[a]

[a] Dr G. Jézéquel, J. Fargier, Dr N. Hue, Dr S. Desrat, Dr F. Roussi
Institut de Chimie des Substances Naturelles
Université Paris-Saclay, CNRS
91198 Gif-sur-Yvette, France
E-mail: fanny.roussi@cnrs.fr

[b] Dr J. Bigay, J. Polidori, Dr B. Antonny
Institut de Pharmacologie Moléculaire et Cellulaire
Université Côte d'Azur, Inserm, CNRS
06560 Valbonne, France

[c] J. Geslin, Pr C. El Kalamouni
Unité Mixte Processus Infectieux en Milieu Insulaire Tropical, Plateforme Technologique CYROI
Université de la Réunion, Inserm, CNRS, IRD
94791 Sainte Clotilde, France

Supporting information for this article is given via a link at the end of the document.

Abstract: The development of innovative antiviral strategies is critical to address the global health threats posed by RNA viruses, including the Zika virus (ZIKV), which can cause severe neurological complications. The lipid transporter OxySterol Binding Protein (OSBP), essential for cholesterol and phosphatidylinositol 4-phosphate trafficking, is exploited by many positive-strand RNA viruses, making it an attractive novel antiviral target. This study investigates simplified analogues of macarangin B, a natural compound with potent OSBP-targeted antiviral activity against ZIKV, but limited stability due to its flavonol moiety. A series of analogues was synthesized, replacing the flavonol with a flavone core while retaining the essential hexahydroxanthene (HHX) motif. These compounds demonstrated improved stability, high OSBP binding affinity, and low cytotoxicity. The most active compounds exhibited antiviral activity comparable to established OSBP inhibitors and were stable in physiologic media, highlighting their potential as leads for therapeutic development. This work advances the structure-activity relationship (SAR) understanding of macarangin B analogues and provides a foundation for designing effective antivirals targeting in ZIKV infections.

Introduction

Emerging and re-emerging RNA viruses, represent a persistent global health threat, demanding innovative antiviral strategies, particularly when vaccines fall short or are unavailable.[1] Among RNA viruses, orthoflavivirus such as Zika virus (ZIKV), dengue virus (DENV), and West Nile virus (WNV) pose significant challenges, as highlighted by the WHO. [2] For example, ZIKV can lead to severe cases of neurological complications, such as Guillain-Barré syndromes in adults and microcephaly in neonates.[3]

These viruses often hijack host pathways including intracellular cholesterol trafficking and endoplasmic reticulum remodeling to establish viral factories critical for their replication. Targeting such host-dependent mechanisms has emerged as a promising strategy to combat viral infections. Recent studies have underscored the Oxysterol Binding Protein (OSBP), a key player in lipid exchange, as an essential factor hijacked by many positive-strand RNA viruses for replication. [4-6]

Several synthetic compounds inhibiting OSBP have already shown antiviral properties, but their lack of selectivity towards the target compromises their development as potential drugs.[7-10] On the other hand, a set of natural compounds, the ORPphilins, including OSW1 and schweinfurthins (SWs), present high affinity towards the target but also an important cytotoxicity that hampers their antiviral application.[11-13] Therefore, while OSBP was identified as a relevant drug target to treat RNA virus infections, there is a lack of compounds showing potential as future drug candidates.

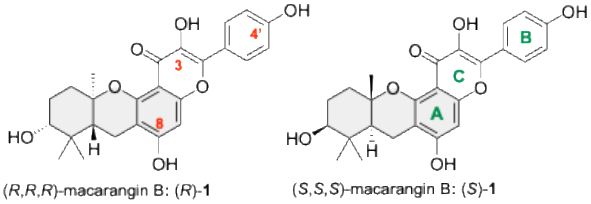

Figure 1. Structure of both enantiomers of natural macarangin B.

In light of these limitations, we recently described macarangin B (**1**), an original racemic natural compound (Figure 1).[14] This compound, particularly its synthetic (*R*,*R*,*R*) enantiomer, displayed excellent selectivity for OSBP, low cytotoxicity and potent antiviral activity against ZIKV. These results paved the way for the development of a new class of antiviral compounds presenting an original mode of action by targeting cholesterol intracellular trafficking. As this molecule's structure is unique, combining a flavonol moiety fused to a hexahydroxanthene (HHX), there is little knowledge about SAR. However, the HHX motif is likely to play a key role, as it is the pharmacophore of SWs that have a high affinity for OSBP.[13] This work presents the synthesis and biological evaluation of simplified analogues of macarangin B (**1**) to expand the structure-activity relationship (SAR) knowledge of this new series. We also aimed at improving its pharmacokinetic properties, with the objective of obtaining a potential hit for antiviral application against Zika virus.

Results and Discussion

Synthesis

The highly promising biological activities of macarangin B (**1**) were slightly hampered by the presence of a flavonol moiety known to be prone to degradation.[15] Hence, to prevent such issues, but also to enrich the SAR knowledge of this new class and facilitate access to active compounds, we set ourselves to the synthesis of simplified analogues. The presence of the 3-hydroxyl is the main reason for chemical and pharmacological instability, as the heterocycle can undergo opening and re-arrangement. Moreover, the more substituted the B-ring is, the higher is the instability.[16]
Thus, we designed analogues of Macarangine B (**1**), also entailing a HHX moiety that was shown to be essential for the activity against OSBP but replacing the flavonol core with a flavone.

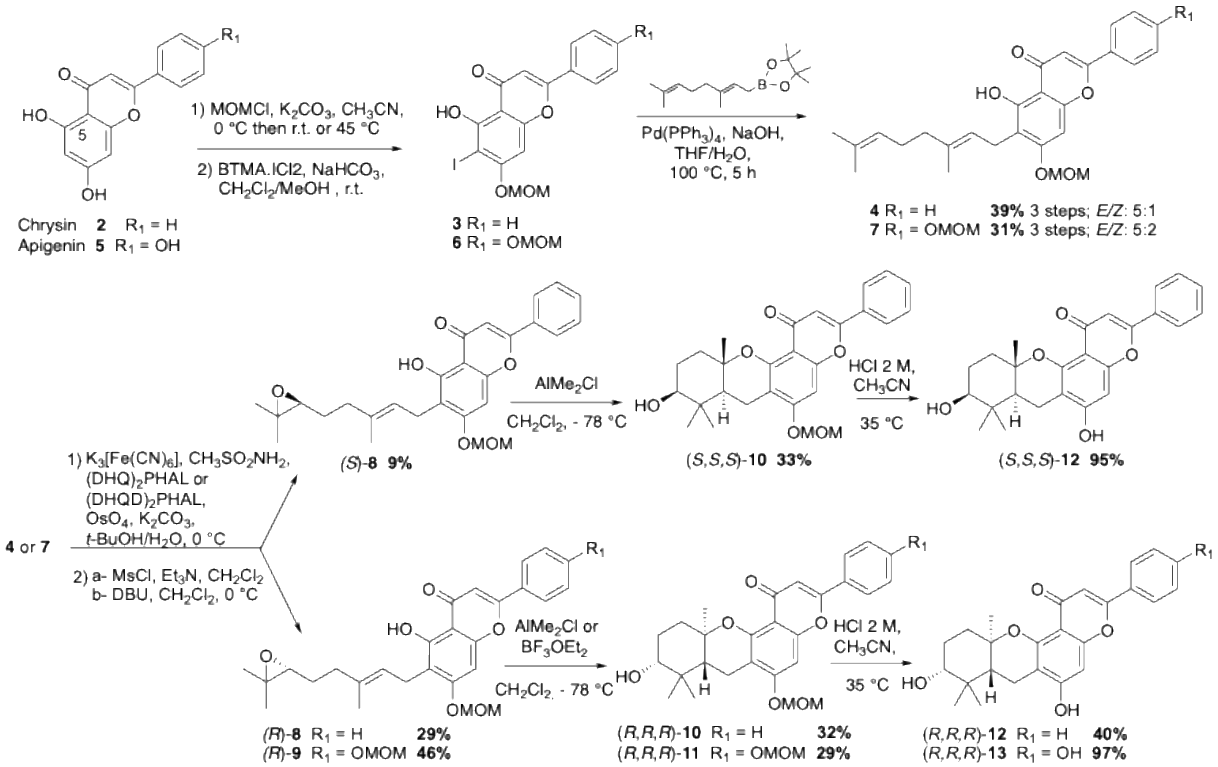

Scheme 1. Synthesis of compounds (*R*,*R*,*R*)-**12** and (*S*,*S*,*S*)-**12** from chrysin **2** and of (*R*,*R*,*R*)-**13** from apigenin

We chose to start the first series from chrysin (**2**). The phenol at C_7 was selectively protected, enabling regioselective iodination at C_6 using benzyltrimethylammonium dichloroiodate ($BTMA{\cdot}ICl_2$) in methanol, which forms methyl hypoiodite to chelate the free phenol at C_5.[17] The resulting iodinated compound **3** underwent Suzuki-Miyaura cross-coupling with geranyl-dioxaborolane, prepared according to described protocol,[18] to yield compound **4** with minimal *E*/*Z* isomerization of the double bond (5:1). From this intermediate, enantioselective dihydroxylation was achieved using Sharpless conditions. Indeed, neither Shi nor Jacobsen methods provided satisfactory results, giving either poor yields or poor enantiomeric excess. The choice of catalyst, $(DHQ)_2PHAL$ or $(DHQD)_2PHAL$, yielded (*R*)- or (*S*)-diols, which were converted to epoxides (*R*)-**8** and (*S*)-**8** *via* mesylation and intramolecular nucleophilic substitution with 1,8-diazabicyclo(5.4.0)undec-7-ene (DBU). Lewis acid-mediated cascade cyclization of these epoxides was then performed using dimethylaluminum chloride (Me_2AlCl) as the optimal catalyst, selected after a screening of a variety of Lewis acid reagents. Expected MOM-protected intermediates (*R*, *R*, *R*)-**10** (*i.e.,* (*R*)-**10**) and (*S*,*S*,*S*)-**10** (*i.e.,* (*S*)-**10**) were obtained with acceptable yields of 32 and 33% after separation of their respective diastereomers arising from the cyclization of (*R*,*Z*)-**8** and (*S,Z*)-**8**. Both (*R*)-**10** and (*S*)-**10** were obtained with excellent enantiomeric *ratios* (*e.r.*) of 94:6 and 97:3, respectively (see Supporting Information). Subsequent phenol deprotection in acidic conditions afforded the desired hexahydroxanthene compounds (*R*,*R*,*R*)-**12** (*i.e.,* (*R*)-**12**) and (*S*,*S*,*S*)-**12** (*i.e.,* (*S*)-**12**) respectively (Scheme 1).

The same synthetic route was successfully applied to apigenin (**5**), another flavone with an additional phenol function on the B-ring (Scheme 2). Protection on the C_7 phenol and regioselective iodination yielded compound **6**, which underwent palladium-catalyzed cross-coupling with geranyl-dioxaborolane to give compound **7**. As expected, the enantioselective dihydroxylation/ mesylation/nucleophilic substitution sequence of compound **7** yielded the epoxide (*R*)-**9**. For this series, the screening of Lewis acids used to induce the cascade polycyclisation giving the hexahydroxanthene derivative (*R*,*R*,*R*)-**11** (*i.e.,* (*R*)-**11**) boron trifluoride diethyl etherate ($BF_3.OEt_2$) was identified as the most efficient one. Final deprotection in acidic conditions of both phenols proceeds in quantitative yield to obtain (*R*,*R*,*R*)-**13** (*i.e.,* (*R*)-**13**).

Biochemical evaluation

OSBP protein, a member of the ORP family, plays a significant role in the intracellular distribution of cholesterol. It is a lipid transporter that operates at membrane contact sites between the endoplasmic reticulum (ER) and the trans-Golgi network (TGN), where it transfers cholesterol in exchange for phosphatidylinositol 4-phosphate (PI4P). Both cholesterol and PI4P bind into the OSBP lipid-binding cavity (ORD domain) in a mutually exclusive manner.[19-21]

We have recently disclosed that macarangin B **1** can bind within the ORD domain of OSBP in place of cholesterol. We used the fluorescence properties of (*R*)- and (*S*)-**1** to determine their apparent affinity (K_d) for the ORD domain, utilizing FRET signals between these compounds and tryptophan residues of the protein.[14]

Replacing the flavonol moiety by a flavone in the chrysin and apigenin chemical series led to the loss of fluorescence properties of the synthesized compounds. To determine the affinity for OSBP of compounds (*R*)- and (*S*)-**10**, (*R*)- and (*S*)-**12**, (*R*)-**11** and (*R*)-**13**, we evaluated their ability to inhibit cholesterol transport using *in vitro* experiments (Figure 2 and Figure S1).[13,19,22]

As previously described, we followed the transfer of dehydroergosterol (DHE) by the ORD domain between two liposome populations in the presence or the absence of each compound. The donor liposomes (La) mimicked the ER and contained DHE, a fluorescent cholesterol analog. The acceptor liposomes mimicked the Golgi (Lb) and contained the fluorescent lipid dansyl PE. Transport of DHE from the donor to the acceptor liposomes was accompanied by a FRET signal between DHE and Dansyl-PE, enabling precise kinetics measurements (Figure 2A). Performing this experiment at eight concentrations for each compound enabled us to determine their apparent inhibitory constant (K*i*) for OSBP, as reported in Figure 2B and Table 1.

As previously described, we followed the transfer of dehydroergosterol (DHE) by the ORD domain between two liposome populations in the presence or the absence of each compound. The donor liposomes (La) mimicked the ER and contained DHE, a fluorescent cholesterol analog. The acceptor liposomes mimicked the Golgi (Lb) and contained the fluorescent lipid dansyl PE. Transport of DHE from the donor to the acceptor Interestingly, in the chrysin series, the protected cyclized compound (*R*)-**10** displayed good activity with a Ki of 17 nM while its enantiomer (*S*)-**10** shows a 50-fold drop in activity. However, regarding deprotected compounds **12**, both enantiomers display an excellent inhibition constant at the single-digit nanomolar range. The apigenin-derived compound (*R*)-**13** shows an interesting inhibition of 13 nM, in the same range as its chrysin analogue (*R*)-**12**. Interestingly, we noticed that the absence of the flavonol moiety does not hinder the affinity of this class of compounds for OSBP. Moreover, (*R*)- protected compounds are also active, although in a lower range than deprotected ones.

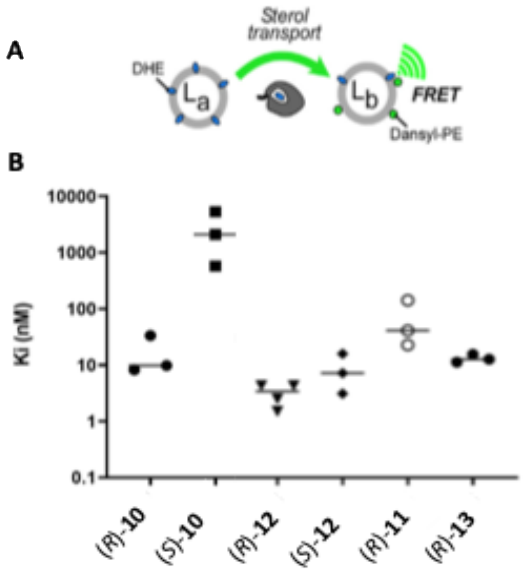

Figure 2. A- Principle of the biochemical assay. B- Inhibitory effect of the indicated compounds on DHE transfer mediated by OSBP ORD domain.

Molecular modelling

We next attempted to rationalize the K*i* values obtained for compounds (*R*)- and (*S*)-**10**, (*R*)- and (*S*)-**12**, (*R*)-**11** and (*R*)-**13** by performing docking simulation into the OSBP-ORD domain (PDB ID: 7v62).[23]

Docking of each newly synthesized compound, macarangin (**1**) and OSW1 was run with AutoDock Vina. In these experiments, the 26 amino acids of the binding site were made flexible. The docked conformations of each compound were clustered based on RMSD and ranked according to binding energy. The ten most favorable binding clusters with the lowest free energies were considered.

As already observed for (*R*)-**1**,[14] two clusters of low-energy poses were obtained for each compound, corresponding to two possible orientations (“up” and “down”) within the ORD pocket: in the “down” orientation, their hexahydroxanthene moiety (HHX) was oriented towards the bottom of the ORD cavity, similarly to the hydroxyl group of cholesterol[23] or OSW1 and in the “up “orientation, their HHX pointed in the direction of the lid. This is a surprising result because chrysin derivatives **10** and **12** do not have a C4’ hydroxyl that could form a hydrogen bond with an amino acid at the bottom of the ORD (directly or through a solvent molecule), such as cholesterol, OSW1, or SWs.

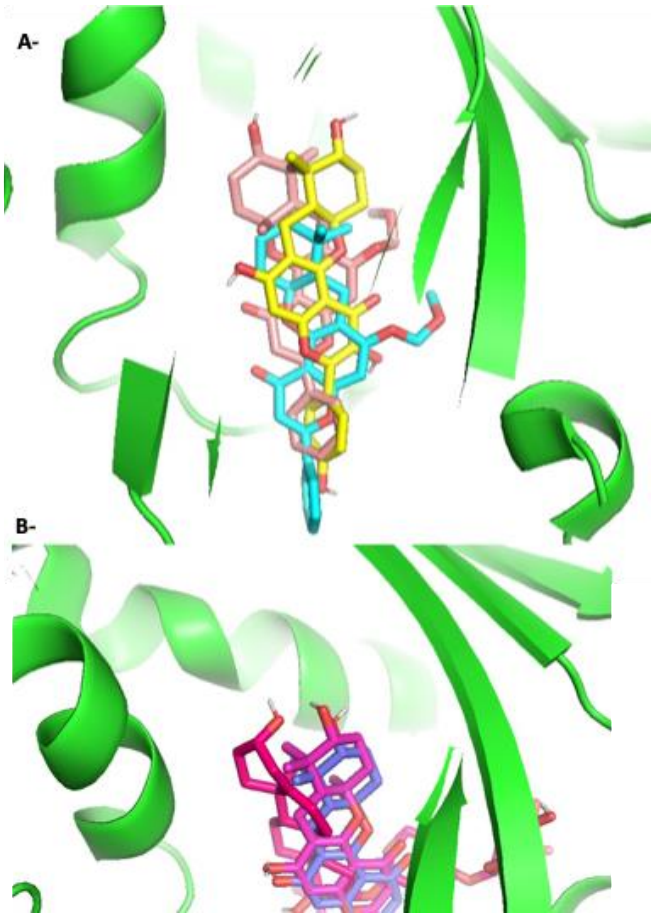

Figure 3. Docking experiments within OSBP-ORD domain (PDB ID: 7v62) using AutoDock Vina. A- Superimposition of the lowest energy conformers of (*R*)-macarangin (**1**) (yellow), (*R*)-**10** (pink) and (*S*)-**10** (cyan), less deeply buried in the pocket. B- Superimposition of the lowest energy conformers of OSW1 (magenta), (*R*)-**12** (violet), and (*R*)-**13** (fushia). Zoom on the hydroxyls that point towards the bottom of the pocket.

In addition, for compounds (*R*)-**10** and *S*-(**12**), a cluster of intermediate positions, *i.e*., perpendicular to the "up" and "down" clusters, was also generated.
The lowest energy conformers of all compounds, except for (S)-**10**, were positioned similarly to those of (*R*)-macarangine (**1**) and OSW1 in the ORD domain, *i.e*., with a down orientation (Figure 3A and 3B). In particular, hydroxyls of the HHX moiety pointed in the same direction as the OSW1 alcohol (Figure 3B). The lowest energy conformer of compound (*S*)-**10** has the same orientation but is higher up in the pocket (Figure 3A).

The 2D visualization of the interaction between all these compounds and the residues of the ORD domain of OSBP provided additional valuable information. The hydroxyl of the HHX The 2D visualization of the interaction between all these compounds and the residues of the ORD domain of OSBP provided additional valuable information. The hydroxyl of the HHX motif, for conformers in the down orientation, does not necessarily make a direct hydrogen bond with an amino acid (see, for example (*R*)-**12** and (*R*)-**13**, Figure 4). On the other hand, all conformers (including the lowest energy conformers of (*R*)-**12**, (*S*)-**12** and (*R*)-**13**, Figure 4) showed crucial π-cation interactions between the flavone or flavonol moiety and one or two amino acids (Arg 449 and potentially Thr 580) as well as additional π-σ or π-alkyl interactions (Lys 493). The 2-phenyl-4*H*-chromen-4-one pattern seems to be more important for interaction with the amino acids in the ORD domain than the hydroxyl at 4', which is not involved in a hydrogen bond and even than the hydroxyl of the HHX moiety.

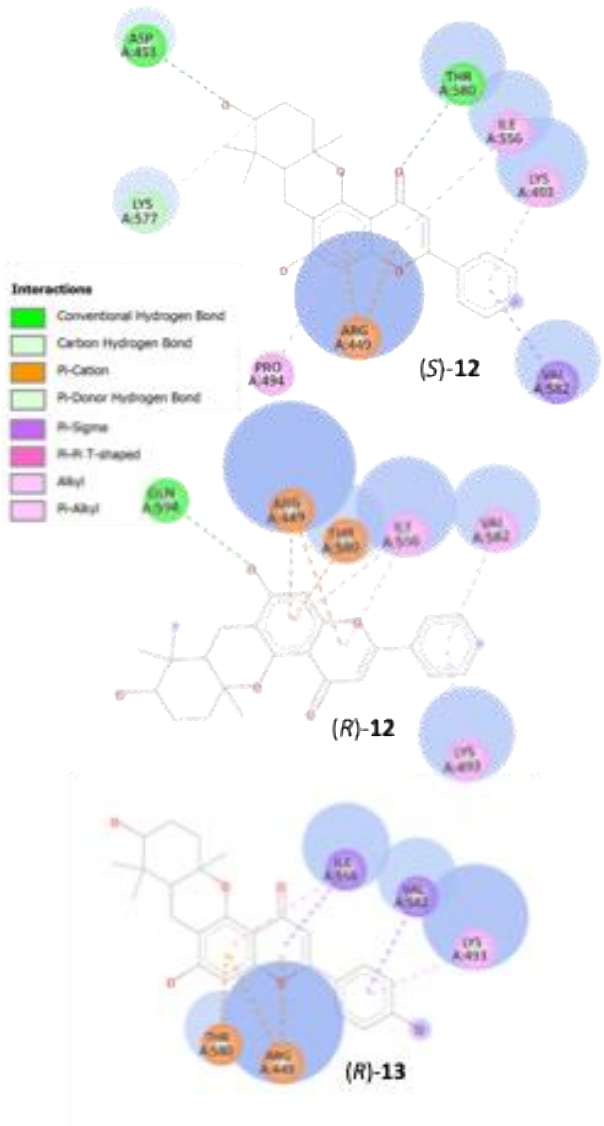

Figure 4. 2D interaction map of compounds (*S*) and (*R*)-**12** and (*R*)-**13** with the amino acids of the ORD domain of OSBP.

Antiviral assay

We next evaluated the antiviral activity of compounds **10**, **12**, (*R*)-**11** and (*R*)-**13** against ZIKV in comparison with (*R*)-**1**, (*S*)-**1**, SW-G and OSW1 (Table 1). A549 cells were infected with ZIKV at multiplicity of infection (MOI) of 1 and incubated for 24 h with We next evaluated the antiviral activity of compounds **10**, **12**, (*R*)-**11** and (*R*)-**13** against ZIKV in comparison with (*R*)-**1**, (*S*)-**1**, SW-G and OSW1 (Table 1). A549 cells were infected with ZIKV at multiplicity of infection (MOI) of 1 and incubated for 24 h with varying concentrations of each compound. ZIKV progeny production was quantified using plaque-forming assay, which measures the number of infectious virus particles released into the supernatant. First, we verified that these compounds were not cytotoxic to A49 cells after 48 h or 72 h of treatment. Under these conditions, only the reference compound OSW1 exhibited a strong cytotoxicity of 70 nM (entry 4). Overall, all the synthesized compounds demonstrated potent antiviral activity at the nanomolar range, with the exception of (*R*)-**12** (entry 7). Notably, compound (*R*)-**10** (entry 5) had an identical IC_{50} of 3 nM to **1** and SW-G (entries 1-3).

Table 1. Effects of compounds **10**, **12**, (*R*)-**11** and (*R*)-**13** on the inhibition of cholesterol transfer, cytotoxicity on A549 cells and antiviral effects on Zika virus.

Entry	Compound	OSBP[a] Ki (nM)	A549[b] CC_{50} (nM)	ZIKV (PFU) [c] IC_{50} (nM)

1	(*R*)-**1**	/	> 20000	4 ± 0.7
2	(*S*)-**1**	/	> 20000	3 ± 0.07
3	SW-G	< 1[d]	> 20000	3 ± 0.01
4	OSW1	ND	70 ±	120 ± 36
5	(*R*)-**10**	17 ± 11	> 20000	3 ± 0.3
6	(*S*)- **10**	2659 ± 1756	> 20000	40 ± 20
7	(*R*)-**12**	4 ± 1.5	> 20000	10860 ± 81
8	(*S*)-**12**	9 ± 5	> 20000	70 ± 40
9	(*R*)-**11**	69 ± 49	> 20000	70 ± 50
10	(*R*)-**13**	13 ± 1.6	> 20000	50 ± 30

[a] Inhibitory effect of the indicated compounds on DHE transfer mediated by OSBP ORD domain. The K*i* of each compound was calculated after three independent experiments. [b] CC_{50}, is the drug concentration required to reduce mitochondrial activity by 50% after 48 h of treatment. It was calculated from three independent experiments. [c] The IC_{50} is the concentration needed to inhibit 50% of viral progeny production after 24 h of incubation and was calculated from three independent experiments. [d] See ref [13].

In vitro stability

As mentioned above, flavonols are unstable over time and natural macarangin A (**1**) showed a tendency to degrade after a few days at room temperature, whereas its protected synthetic precursor (*R*)-**14**[14] could be stored for months without decomposing. Having synthesized flavone analogues that showed promising activity both on the target and on cells infected with the Zika virus, we wanted to assess their potential for further lead development. Therefore, we performed *in vitro* stability measurements in mouse plasma and microsomes to compare the stability in physiologic media of compounds (*R*)-**12** and (*R*)-**13** with that of (*R*)-**14** (Table 2 and Figure S1).

Both compounds (*R*)-**12** and (*R*)-**13** were stable in mouse plasma, contrary to (*R*)-**14** which has a half-life of 16 h (Figure S1). In addition, compound (*R*)-**13** was the only one that presented a moderate in vitro intrinsic clearance of 26 µL/min/mg protein, *i.e.*, below 48 µL/min/mg protein, whereas (*R*)-**14** and (*R*)-**12** were promptly metabolized by hepatic enzymes and had a high clearance (52 and 152 µL/min/mg protein respectively). Interestingly, we also monitored the potential products formed by the metabolization of (*R*)-**12**, and could quantify the concomitant apparition of compound (*R*)-**13** (Figure S1). Compound (*R*)-**12** therefore is metabolized by the CYP450 to its hydroxylated analogue (*R*)-**13**, which is stable in these experimental conditions, and active on the binding and antiviral assays.

Table 2. *In vitro* stability assays for compounds (*R*)-**12**, (*R*)-**13** compared to that of (*R*)-**14**,[14], a stable precursor of macarangin B (**1**).

***In vitro* mouse plasma stability**			
Compound	(*R*)-**14**	(*R*)-**12**	(*R*)-**13**
Metabolic stability (%) [a]	90	99	100
Half-life	16 h	-	-
***In vitro* mouse microsomal stability**			
Compound	(*R*)-**14**	(*R*)-**12**	(*R*)-**13**
Metabolic stability (%)[b]	30	3	64
In vitro intrinsic clearance (µL/min/mg protein)	52	152	26
Metabolic stability (%) non-NADPH dependent	99	88	100

Metabolites	unknown	(*R*)-**13** +?	unknown

[a] at t = 120 min. [b] at t = 45 min.

Conclusion

In summary, we have elaborated simplified analogues of macarangin B (1) that target the OSBP protein and exhibit promising antiviral properties. This study has enabled us to carry out initial SAR studies confirming the value of this type of compounds. Among all the derivatives synthesized, compound (R)-13 stands out as the most promising candidate, combining nanomolar affinity for OSBP, potent anti-ZIKV activity, very good metabolic stability and low clearance. In fine, this compound is the best hit and will serves as a robust starting point for a hit-to-lead optimization strategy in the fight against orthoflavivirus.

Experimental Section

Chemistry

All reagents and solvents were used as purchased from commercial suppliers. Purifications by column chromatography on silica gel were performed using Merck Silica Gel 60 (70–230 mesh). ^{1}H and ^{13}C NMR spectra were recorded on Bruker ARX500 instruments using DMSO-d_6, MeOD, or CD_3CN as internal reference. Chemical shifts (δ values) are given in parts per million (ppm), and the multiplicity of signals are reported as follows: s, singlet; bs, broad singlet; d, doublet; t, triplet; q, quartet; dd, doublet of doublets; m, multiplet. HRMS analyses were performed using a Waters LCT Premier instrument by ElectroSpray Ionization (ESI). IR spectra were recorded on a PerkinElmer Spectrum BX-FTIR spectrometer.

***5-hydroxy-6-iodo-7-(methoxymethoxy)-2-phenyl-4H-chromen-4-one* 3.** A mixture of chrysin **2** (12.0 g, 47.2 mmol, 1 eq) and K_2CO_3 (19.6 g, 141.6 mmol, 3 eq) in acetonitrile (150 mL) was placed under argon and cooled down to 0 °C. MOMCl (4.1 mL, 61.4 mmol, 1.3 eq) was added dropwise for 1.5 h and the mixture was stirred at room temperature until the completion of the reaction. It was then quenched with water (200 mL) and buffered to pH 4 with a solution of HCl 2 M. The mixture was extracted twice with methyl *t*-butyl ether and then with a mixture of EtOAc/*i*-PrOH (3:1). The combined organic phases were washed with brine, dried over $MgSO_4$, and concentrated under reduced pressure. The crude mixture (13.8 g) was directly engaged in the next step except for a sample that was purified by column chromatography on silica gel using heptane/EtOAc 95:5 to 0:100 to enable chemical analysis of pure 5-hydroxy-7-(methoxymethoxy)-2-phenyl-4H-chromen-4-one. ^{1}H NMR (500 MHz, acetone-d_6): δ 12.84 (s, 1 H, OH), 8.09 (dd, J = 7.9, 1.5 Hz, 2 H), 7.63-7.60 (m, 3 H), 6.84 (s, 1H), 6.81 (d, J = 2.2 Hz, 1 H), 6.44 (d, J = 2.3 Hz, 1 H), 5.34 (s, 2 H), 3.49 (s, 3 H) ppm; ^{13}C NMR (500 MHz, acetone-d_6): δ 183.5, 165.2, 164.3, 163.1, 158.7, 132.9, 132.3, 130.1 (2 C), 127.4 (2 C), 106.9, 106.4, 100.6, 95.5, 95.3, 56.7 ppm; HRMS (ESI): *m/z* calcd. for $C_{17}H_{15}O_5^+$ $[M+H]^+$ 299.0914; found 299.0916; IR: *v* 1654, 1613, 1508, 1149, 1078, 1028 cm^{-1}. The previous crude reaction (46.4 mmol), $NaHCO_3$ (19.5 g, 231.8 mmol, 5 eq) and $BTMA.ICl_2$ (15.3 g, 44.0 mmol, 0.95 eq) were solubilized in 300 mL of a mixture of DCM/MeOH (2:1) and placed under argon. The reaction was stirred at room temperature in the dark for 3 h, after which it was quenched slowly at 0 °C with 1 M HCl. The mixture was extracted 2 times with a solution of DCM/MeOH (95:5) and then twice with a solution of EtOAc/isopropanol (3:1). The combined organic phases were dried over $MgSO_4$ and concentrated under reduced pressure. The crude mixture was purified by column chromatography on silica gel using heptane/AcOEt 95:5 to 0:100 to give compound **3** as a pale-yellow solid (13.3 g, 67% over two steps). ^{1}H NMR (500 MHz, CD_3CN): δ 13.86 (s, 1 H, OH), 8.01 (d, J = 7.3 Hz, 2 H), 7.61 (d, J = 7.3 Hz, 1 H), 7.58 (dd, J = 14.6, 6.5 Hz, 2 H), 6.92 (s, 1H), 6.84 (s, 1 H), 5.38 (s, 2 H), 3.52 (s, 3 H) ppm; ^{13}C NMR (500 MHz, CD_3CN): δ 183.2, 165.9, 162.5, 162.5, 159.3, 133.3, 132.2, 130.3 (2C), 127.69 (2C), 107.7, 106.6, 96.4, 94.9, 71.6, 57.5 ppm; HRMS (ESI): *m/z* calcd. for $C_{17}H_{15}O_5^+$ $[M+H]^+$ 424.9880; found 424.9883; IR: *v* 1649, 1599, 1480, 1450, 1345, 1052 cm^{-1}.

***(E)-6-(3,7-dimethylocta-2,6-dien-1-yl)-5-hydroxy-7-(methoxymethoxy)-2-phenyl-4H-chromen-4-one* 4.** NaOH (306 mg, 7.66 mmol, 2.5 eq) and $Pd(PPh_3)_4$ (48 mg, 0.03 mmol, 0.01 eq) were added to a solution of **4** (1.30 g, 3.06 mmol) and geranyl boronic ester (1.21 g, 4.60 mmol, 1.5 eq) in 16 mL of a degassed mixture of THF/water (1:1). The resulting mixture

was stirred at 100 °C in a microwave for approximately 5 h. When the reaction was completed (TLC monitoring), the mixture was filtrated on a pad of Celite and extracted 3 times with EtOAc. The combined organic phases were washed with brine, dried over $MgSO_4$, filtrated and concentrated. The crude mixture was purified by column chromatography on silica gel using heptane/EtOAc 95:5 to 0:100 to give the desired compound **4** (*E*/*Z* 5:1 inseparable mixture) as a pale-yellow oil (774 mg, 1.78 mmol, 58%). HRMS (ESI): *m/z* calcd. for $C_{27}H_{31}O_5^+$ $[M+H]^+$ 435.2166 ; found 435.2165; *E* isomer: ^{1}H NMR (500 MHz, CD_3CN): *δ* 13.04 (s, 1 H, OH), 8.00 (d, *J* = 7.9 Hz, 2 H), 7.59 (d, *J* = 6.6 Hz, 1 H), 7.57 (dd, *J* = 13.6, 6.1 Hz, 2 H), 6.82 (s, 1 H), 6.76 (s, 1 H), 5.32 (s, 2 H), 5.23 (t, *J* = 8.4 Hz, 1 H), 5.06 (t, *J* = 8.4 Hz, 1 H), 3.47 (s, 3 H), 3.36 (d, *J* = 7.6 Hz, 2 H), 2.26 (t, *J* = 8.4 Hz, 1 H), 2.14 (t, *J* = 8.6 Hz, 1 H), 2.04 (t, *J* = 7.3 Hz, 1 H), 1.98 (d, *J* = 8.6 Hz, 1 H), 1.80 (s, 3 H), 1.61 (s, 3 H), 1.55 (s, 3 H) ppm; ^{13}C NMR (125 MHz, CD_3CN): *δ* 183.9, 165.2, 161. 8, 159.5, 157.0, 136.4, 133.0, 132.4 (2 C), 130.2 (2 C), 127.5 (2 C), 125.3, 122.9, 114.3, 106.8, 106.6, 95.3, 93.7, 57.0, 40.5, 27.5, 25.9, 22.1, 17.8, 16.4 ppm; *Z* isomer: ^{1}H NMR (500 MHz, CD_3CN): *δ* 13.04 (s, 1 H, OH), 8.00 (d, *J* = 7.9 Hz, 2 H), 7.59 (d, *J* = 6.6 Hz, 1 H), 7.57 (m, 2 H), 6.82 (s, 1 H), 6.76 (s, 1 H), 5.32 (s, 2 H), 5.23 (t, *J* = 8.4 Hz, 1 H), 5.06 (t, *J* = 8.4 Hz, 1 H), 3.47 (s, 3 H), 3.36 (d, *J* = 7.6 Hz, 2 H), 2.26 (t, *J* = 8.4 Hz, 1 H), 2.14 (t, *J* = 8.6 Hz, 1 H), 2.04 (t, *J* = 7.3 Hz, 1 H), 1.98 (d, *J* = 8.6 Hz, 1H), 1.69 (s, 3 H), 1.67 (s, 3 H), 1.64 (s, 3 H) ppm; HRMS (ESI): *m/z* calcd. for $C_{27}H_{31}O5^+$ $[M + H]^+$: 435.2166; found: 435.2165; IR: *v* 2921, 1655, 1616, 1453, 1343, 1154, 1061 cm^{-1}.

5-hydroxy-6-iodo-7-(methoxymethoxy)-2-(4-(methoxymethoxy)phenyl)-4*H*-chromen-4-one 6. A mixture of apigenin **5** (1.04 g, 3.9 mmol, 1 eq) and K_2CO_3 (2.13 g, 15.4 mmol, 4 eq) in acetonitrile (39 mL) was heated to 45 °C for 1 h. The mixture was then cooled to room temperature, and MOMCl (0.49 mL, 7.3 mmol, 1.9 eq) was added dropwise for 2.5 h. When the reaction was complete, the mixture was quenched with HCl 2M (15 mL). The reaction mixture was extracted 3 times with EtOAc and washed with brine. The combined organic phases were dried over $MgSO_4$ and concentrated under reduced pressure. The crude mixture was purified by column chromatography on silica gel using Heptane/EtOAc 95:5 to 0:100 to give 5-hydroxy-7-(methoxymethoxy)-2-(4-(methoxymethoxy) phenyl)-4H-chromen-4-one as a pale-yellow solid (644 mg, 47%). ^{1}H NMR (500MHz, CD_3CN): *δ* 12.84 (s, OH, 1 H), 7.96 (d, *J* = 8.5 Hz, 2 H), 7.18 (d, *J* = 8.5 Hz, 2 H), 6.74 (d, *J* = 2.2 Hz, 1 H), 6.66 (s, 1 H), 6.43 (d, *J* = 2.2 Hz, 1 H), 5.28 (s, 2 H), 5.27 (s, 2 H), 3.48 (s, 3 H), 3.46 (s, 3 H) ppm; ^{13}C NMR (125 MHz, CD_3CN): *δ* 183.7, 165.4, 164.3, 163.1, 161.5, 158.9, 129.4 (2 C), 125.6, 117.3 (2 C), 107.1, 105.5, 100.6, 95.6, 95.5, 95.4, 57.0, 56.7 ppm; HRMS (ESI): *m/z* calcd. for $C_{19}H_{19}O_7^+$ $[M+H]^+$ 359.1053; found: 359.1133; IR: *v* 2984, 1654, 1603, 1586, 1154; 1144, 1072, 986 cm^{-1}. The preceding compound was iodinated with $BTMA.ICl_2$ (see above protocol) to give compound **6**, which was found to be sufficiently pure to proceed to the next step without purification. ^{1}H NMR (500 MHz, CD_3CN): *δ* 13.96 (s, 1 H, OH), 7.96 (d, *J* = 8.50 Hz, 2 H), 7.18 (d, *J* = 8.5 Hz, 2 H), 6.89 (s, 1 H), 6.75 (s, 1H), 5.37 (s, 2 H), 5.27 (s, 2 H), 5.14 (s, 2 H), 3.50 (s, 3 H), 3.45 (s, 1 H), 3.21 (s, 3 H) ppm.

(*E*)-6-(3,7-dimethylocta-2,6-dien-1-yl)-5-hydroxy-7-(methoxymethoxy)-2-(4(methoxymethoxy)phenyl) -4*H*-chromen-4-one 7. Following the same procedure as for the synthesis of compound **4**, compound **7** (*E/Z* 5:2 inseparable mixture) was obtained with 67% yield over 2 steps. *E* isomer: ^{1}H NMR (500 MHz, CD_3CN): *δ* 13.06 (s, 1 H, OH), 7.87 (d, *J* = 8.8 Hz, 2 H), 7.12 (dd, *J* = 8.8 Hz, 2 H), 6.71 (s, 1 H), 6.58 (s, 1 H), 5.28 (s, 2 H), 5.24 (s, 2 H), 5.20 (t, *J* = 6.7 Hz, 1 H), 5.05 (t, *J* = 6.7 Hz, 1 H), 3.45 (s, 6 H), 3.30 (d, *J* = 6.7 Hz, 2 H), 2.06–2.01 (m, 2 H), 1.99–1.94 (m, 2 H), 1.77 (s, 3 H), 1.60 (s, 3 H), 1.54 (s, 3 H) ppm; ^{13}C NMR (125 MHz, CD_3CN): *δ* 183.5, 164.8, 161.4, 161.2, 159.3, 156.7, 136.2, 132.1, 129.1 (2 C), 125.4, 125.2, 122.9, 117.4 (2 C), 114.0, 106.5, 105.1, 95.2, 95.1, 93.4, 56.9, 56.6, 40.4, 27.4, 25.8, 22.1, 17.7, 16.3 ppm; *Z* isomer: ^{1}H NMR (500 MHz, CD_3CN): *δ* 13.05 (s, 1 H, OH), 7.87 (d, *J* = 8.8 Hz, 2 H), 7.12 (d, *J* = 8.8 Hz, 2 H), 6.71 (s, 1 H), 6.58 (s, 1 H), 5.28 (s, 2 H), 5.24 (s, 2 H), 5.20 (t, *J* = 6.7 Hz, 1 H), 5.05 (t, *J* = 6.7 Hz, 1 H), 3.50 (d, *J* = 6.7 Hz, 2 H), 3.45 (s, 6 H), 2.26–2.21 (m, 2 H), 2.13–2.08 (m, 2 H), 1.68 (s, 3 H), 1.66 (s, 3 H), 1.63 (s, 3 H) ppm; ^{13}C NMR (125 MHz, CD_3CN): *δ* 183.5, 164.8, 161.4, 161.2, 159.3, 156.7, 136.6, 132.3, 129.1 (2 C), 125.4, 125.4, 123.6, 117.4 (2 C), 114.0, 106.5, 105.1, 95.2, 95.1, 93.4, 56.9, 56.6, 32.6, 27.4, 25.9, 23.6, 22.0, 17.8 ppm; HRMS (ESI): *m/z* calcd. for $C_{29}H_{35}O_7^+$ $[M+H]^+$ 495.2377; found: 495.2372; IR: *v* 2911, 1654, 1606, 1484, 1449, 1342, 1244, 1179, 1152, 1059, 984, 835 cm^{-1}.

(*R*,*E*)-6-(5-(3,3-dimethyloxiran-2-yl)-3-methylpent-2-en-1-yl)-7-(methoxymethoxy)-4-oxo-2-phenyl-4*H*-chromen-5-yl acetate (*R*)-8. Compound **4** (509 mg, 1.17 mmol) was dissolved in a 2:1 mixture of *t*-BuOH and water (13 mL). K_2CO_3 (648 mg, 4.69 mmol, 4 eq), K_3FeCN_6 (964 mg, 2.93 mmol, 2.5 eq), $(DHQ)_2PHAL$ (36 mg, 0.05 mmol, 0.04 eq), OsO_4 4 % in water (0.30 mL, 0.05 mmol, 0.04 eq) and methanesulfonamide (145 mg, 1.52 mmol, 1.3 eq) were successively added. The reaction mixture was stirred at 0 °C for 16 h and quenched with an aqueous solution of Na_2SO_3 (369 mg, 2.93 mmol, 2.5 eq). The reaction mixture was extracted 3 times with EtOAc. The combined organic phases were washed with brine, dried over $MgSO_4$, filtrated and concentrated under reduced pressure. The crude mixture was purified by column chromatography on silica gel (gradient of heptane and EtOAc with 1% AcOH) to give (*S*)-6-(6,7-dihydroxy-3,7-dimethyloct-

2-en-1-yl)-5-hydroxy-7-(methoxymethoxy)-2-phenyl-4*H*-chromen-4-one (*E/Z* 5:1 inseparable mixture) as a pale-yellow oil (293 mg, 0.63 mmol, 53%). *E isomer*: ^{1}H NMR (500 MHz, CD_3CN): *δ* 13.04 (s, 1 H, OH), 8.00 (d, 2 H, J = 7.9 Hz), 7.60–7.56 (m, 3 H), 6.82 (s, 1 H), 6.76 (s, 1 H), 5.33 (s, 2 H), 5.26 (t, *J* = 6.6 Hz, 1 H), 3.47 (s, 3 H), 3.38 (d, *J* = 6.8 Hz, 2 H), 3.15 (dd, *J* = 10.0, 5.0 Hz, 1 H), 2.72 (d, *J* = 4.7 Hz, 1 H, OH), 2.57 (s, 1 H, OH), 2.23–1.94 (m, 4 H), 1.80 (s, 3 H), 1.05 (s, 3 H), 1.04 (s, 3 H) ppm; ^{13}C NMR (500 MHz, CD_3CN): *δ* 183.8, 165.1, 161.6, 159.4, 156.9, 136.7, 132.9, 132.3, 130.1 (2 C), 127.4 (2 C), 122.8, 114.3, 106.8, 106.5, 95.2, 93.7, 78.6, 73.1, 56.9, 37.6, 30.7, 26.1, 24.6, 22.2, 16.4 ppm; *Z isomer*: ^{1}H NMR (500 MHz, CD_3CN): *δ* 13.04 (s, 1H, OH), 8.00 (d, *J* = 7.9 Hz, 2 H), 7.60–7.56 (m, 3 H), 6.82 (s, 1 H), 6.76 (s, 1 H), 5.33 (s, 2 H), 5.26 (t, *J* = 6.6 Hz, 1 H), 3.47 (s, 3 H), 3.38 (d, *J* = 6.8 Hz, 2 H), 3.15 (dd, *J* = 10.0, 5.0 Hz, 1 H), 2.72 (d, *J* = 4.7 Hz, 1 H, OH), 2.57 (s, 1 H, OH), 2.23–1.94 (m, 4 H), 1.67 (s, 3 H), 1.11 (s, 3 H), 1.09 (s, 3 H) ppm; $[\alpha]_{20}^{D}$ +6.9 ° (*c* 0.5 in CH_3CN). HRMS (ESI): *m/z* calcd. for $C_{27}H_{33}O_7^+$ $[M+H]^+$ 469.2221; found 469.2215. Freshly distillated triethylamine (0.33 mL, 2.43 mmol, 4 eq) was added, at 0 °C under argon, to a solution of the (*S*)-diol (0.61 mmol) in 3.4 mL of anhydrous dichloromethane. The mixture was stirred at 0 °C for 30 min, then MsCl (0.09 mL, 1.21 mmol, 2 eq) was added and the mixture was stirred again for 30 min. When the mesylation was completed (TLC monitoring), DBU (1.09 mL, 7.27 mmol, 12 eq) was added and the mixture was stirred for 3 h at the same temperature. After completion of the reaction, a saturated solution of NH_4Cl was added and the mixture was warmed to room temperature. The organic phase was decanted and the aqueous phase was extracted 3 times with EtOAc. The combined organic phases were washed with water, dried over $MgSO_4$, filtrated and concentrated. The crude product was purified by column chromatography on silica gel using Heptane/EtOAc 95:5 to 0:100 to obtain compound (*R*)-**8** (E/Z 5:1 inseparable mixture) as a pale-yellow oil (151 mg, 0.34 mmol, 29% over 3 steps. *E* isomer: ^{1}H NMR (500 MHz, CD_3CN): *δ* 13.00 (s, 1 H), 7.92 (d, *J* = 7.7 Hz, 2 H), 7.56–7.49 (m, 3 H), 6.73 (s, 1 H), 6.67 (s, 1 H), 5.28 (s, 2 H), 5.25 (t, *J* = 7.2 Hz, 1 H), 3.45 (s, 3 H), 3.31 (d, *J* = 7.6 Hz, 2 H), 2.58 (t, *J* = 6.4 Hz, 1 H), 2.10–2.05 (m, 2 H), 1.79 (s, 3 H), 1.59–1.51 (m, 2 H), 1.15 (s, 3 H), 1.13 (s, 3 H) ppm; ^{13}C NMR (500 MHz, CD_3CN): *δ* 183.6, 164.9, 161.6, 159.3, 156.8, 135.6, 132.8, 132.2, 130.0 (2 C), 127.3 (2 C), 123.3, 114.0, 106.6, 106.4, 95.2, 93.5, 64.5, 58.7, 56.9, 37.0, 28.1, 25.0, 22.2, 18.9, 16.3 ppm; *Z* isomer: ^{1}H NMR (500 MHz, CD_3CN): *δ* 13.00 (s, 1 H, OH), 7.92 (d, *J* = 7.7 Hz, 2 H), 7.56–7.49 (m, 3 H), 6.73 (s, 1 H), 6.67 (s, 1 H), 5.28 (s, 2 H), 5.25 (t, *J* = 7.2 Hz, 1 H), 3.45 (s, 3 H), 3.31 (*d*, *J* = 7.6 Hz, 2 H), 2.58 (t, *J* = 6.4 Hz, 1 H), 2.10–2.05 (m, 2 H), 1.68 (s, 3 H), 1.59–0.51 (m, 2 H), 1.27 (s, 3 H), 1.26 (s, 3 H) ppm; $[\alpha]_{20}^{D}$ -5.3 ° (*c* 1.0 in CH_3CN); HRMS (ESI): *m/z* calcd. for $C_{27}H_{31}O_6^+$ $[M+H]^+$ 451.2115; found 451.2119; IR: *v* 2927, 1638, 1602, 1451, 1345, 1153, 1046, 926 cm^{-1}.

(*S*,*E*)-6-(5-(3,3-dimethyloxiran-2-yl)-3-methylpent-2-en-1-yl)-7-(methoxymethoxy)-4-oxo-2-phenyl-4*H*-chromen-5-yl acetate (*S*)-8. The same procedure using $(DHQD)_2PHAL$ as catalyst in the first step. Compound (*S*)-**8** (*E/Z* 5:1 inseparable mixture) was obtained with 9% yield over 3 steps $[\alpha]_{20}^{D}$ +4.5° (*c* 1.0 in CH_3CN).

(*R*,*E*)-6-(5-(3,3-dimethyloxiran-2-yl)-3-methylpent-2-en-1-yl)-5-hydroxy-7-(methoxymethoxy)-2-(4 (methoxymethoxy)phenyl)-4*H*-chromen-4-one (*R*)-9. Same procedure as for the formation of compound (*R*)-**8**, starting from **7**. Compound (*R*)-**9** (*E/Z* 5:2 inseparable mixture) was obtained with 46% yield over 3 steps. *E* isomer: ^{1}H NMR (500 MHz, CD_3CN): *δ* 13.04 (s, 1 H, OH), 7.85 (d, *J* = 8.3 Hz, 2 H), 7.11 (d, *J* = 8.3 Hz, 2 H), 6.70 (s, 1 H), 6.56 (s, 1 H), 5.27 (s, 2 H), 5.25 (m, 1 H), 5.24 (s, 2 H), 3.45 (s, 3 H), 3.44 (s, 3 H), 3.30 (d, *J* = 6.6 Hz, 2 H), 2.58 (t, *J* = 5.8 Hz, 1 H), 2.13–2.02 (m, 2 H), 1.79 (s, 3 H), 1.64–1.50 (m, 2 H), 1.15 (s, 3 H), 1.13 (s, 3 H) ppm; ^{3}C NMR (125 MHz, CD_3CN): *δ* 183.5, 164.7, 161.4, 161.1, 159.3, 156.7, 135.6, 129.0 (2 C), 125.3, 123.3, 117.4 (2 C), 113.9, 106.4, 105.0, 95.3, 95.2, 93.4, 64.5, 58.7, 56.9, 56.6, 37.0, 28.1, 24.9, 23.5, 18.9, 16.3 ppm; *Z* isomer: ^{1}H NMR (500 MHz, CD_3CN): *δ* 13.05 (s, 1 H, OH), 7.85 (d, *J* = 8.3 Hz, 2 H), 7.11 (d, *J* = 8.3 Hz, 2 H), 6.54 (s, 1 H), 6.43 (s, 1 H), 5.27 (s, 2 H), 5.25 (m,1 H), 5.24 (s, 2 H), 3.45 (s, 3 H), 3.44 (s, 3 H), 3.30 (d, *J* = 6.6 Hz, 2 H), 2.73 (t, *J* = 6.2 Hz, 1 H), 2.13–2.02 (m, 2 H), 1.67 (s, 3 H), 1.64–1.50 (m, 2 H), 1.27 (s, 3 H), 1.26 (s, 3 H) ppm; ^{13}C NMR (125 MHz, CD_3CN): *δ* 183.5, 164.7, 161.4, 161.1, 159.2, 156.7, 135.9, 129.0 (2 C), 125.3, 123.9, 117.4 (2 C), 113.8, 106.4, 105.0, 95.3, 95.2, 93.4, 64.6, 58.8, 56.9, 56.6, 36.9, 28.3, 25.1, 22.2, 19.0, 16.5 ppm; $[\alpha]_{20}^{D}$ -1.3 ° (*c* 1.5 in CH_3CN); HRMS (ESI): *m/z* calcd. for $C_{29}H_{35}O_8^+$ $[M+H]^+$ 511.2326; found: 511.2326; IR: *v* 2958, 2924, 1739, 1652, 1606, 1509, 1486, 1450, 1342, 1240, 1178, 1061, 986, 837 cm^{-1}.

(7a*R*,9*R*,11a*R*)-9-hydroxy-6-(methoxymethoxy)-8,8,11a-trimethyl-3-phenyl-7a,8,9,10,11,11a-hexahydro-1*H*,7*H*-pyrano[2,3-*c*]xanthen-1-one (*R,R,R*)-10. A solution of *(R)*-**8** (95 mg, 0.2 mmol, 1 eq) in anhydrous dichloromethane (4 mL) under argon was cooled to -78 °C. Me_2AlCl (0.63 mL, 1 M in hexanes, 0.6 mmol, 3 eq) was then added dropwise, and the mixture was stirred for 1 h at -78 °C. The reaction was quenched with a solution of HCl 2M (0.3 mL), then $MgSO_4$ was added and the mixture was filtrated, and concentrated under reduced pressure. The product was purified by column chromatography on silica gel using heptane/EtOAc 95:5 to 0:100 with 1% of acetic acid to give *(R, R, R)*-**10** (30 mg, 32%) as a yellow oil. ^{1}H NMR (500 MHz, CD_3CN): *δ* δ 7.94 (dd, *J* = 7.6 Hz, 2 H), 7.55–7.51 (m, 3 H), 6.80 (s, 1 H), 6.51 (s, 1 H), 5.33 (s, 2 H), 3.50 (s, 3 H), 3.39–3.33 (m, 1 H), 2.78 (dd, *J* = 17.0, 5.1 Hz, 1 H), 2.76 (s, 1 H), 2.45 (dd, *J* = 17.0, 13.4 Hz,

1 H), 2.03 (dt, *J* = 12.1, 3.0 Hz, 1 H), 1.82–1.74 (m, 2 H), 1.64–1.58 (m, 2 H), 1.21 (s, 3 H), 1.07 (s, 3 H), 0.86 (s, 3 H) ppm; ^{13}C NMR (125 MHz, CD_3CN): δ 177.3, 161.3, 160.0, 158.8, 154.8, 132.8, 132.2, 130.0 (2 C), 127.0 (2 C), 110.3, 109.9, 109.5, 95.4, 94.6, 78.6, 78.0, 57.0, 46.5, 39.3, 38.6, 29.1, 27.7, 20.2, 18.9, 14.9 ppm; $[\alpha]_{20}^{D}$ +60.3 ° (*c* 0.4 in CH_3CN); HRMS (ESI): *m/z* calculated for $C_{27}H_{31}O_6^+$ $[M + H]^+$: 451.2115; found: 451.2061. IR: *v* 3363, 2942, 1633, 1595, 1450, 1347, 1095, 1056, 1035, 908 cm^{-1}.

(7a*S*,9*S*,11a*S*)-9-hydroxy-6-(methoxymethoxy)-8,8,11a-trimethyl-3-phenyl-7a,8,9,10,11,11a-hexahydro-1*H*,7*H*-pyrano[2,3-*c*]xanthen-1-one (*S,S,S*)-10. The same procedure as above to yield (*S*,*S*,*S*)-**10** (33%). $[\alpha]_{20}^{D}$ -68.0 ° (*c* 0.8 in CH_3CN).

(7a*R*,9*R*,11a*R*)-9-hydroxy-6-(methoxymethoxy)-3-(4-(methoxymethoxy)phenyl)-8,8,11a-trimethyl-7a,8,9,10,11,11a-hexahydro-1*H*,7*H*-pyrano[2,3-*c*]xanthen-1-one (*R*,*R*,*R*)-11. Compound (*R*)-**9** (31 mg, 0.06 mmol, 1 eq) was solubilized in anhydrous dichloromethane (3 mL) under argon and cooled to -78 °C. A 10% solution of $BF_3{\cdot}OEt_2$ (0.12 mmol, 2 eq) in anhydrous dichloromethane (0.15 mL) was then added dropwise, and the mixture was stirred for 30 min at -78 °C. The reaction was quenched with 1 mL of water and extracted 3 times with dichloromethane. The combined organic phases were washed with water, dried over $MgSO_4$ and concentrated under reduced pressure. The crude product was purified by preparative TLC, using heptane/EtOAc/acetic acid 2:8:0.1 to give pure compound 15 (9 mg, 29%) as a yellow oil. ^{1}H NMR (500 MHz, CD_3CN): *δ* 7.88 (d, *J* = 8.4 Hz, 2 H), 7.14 (d, *J* = 8.7 Hz, 2 H), 6.77 (s, 1 H), 6.42 (s, 1 H), 5.32 (s, 2 H), 5.25 (s, 2 H), 3.49 (s, 3 H), 3.44 (s, 3 H), 3.38–3.32 (m, 1 H), 3.18 (s, 3 H), 2.77 (dd, *J* = 15.8, 6.3 Hz, 1 H), 2.76 (s, 1 H, OH), 2.44 (dd, *J* = 17.4, 14.3 Hz, 1 H), 2.05–2.00 (m,1 H), 1.83–1.73 (m, 2 H), 1.65–1.58 (m, 2 H), 1.20 (s, 3 H), 1.07 (s, 3 H), 0.86 (s, 3 H) ppm; ^{13}C NMR (125 MHz, CD_3CN): *δ* 177.3, 161.0, 160.5, 159.8, 158.6, 154.7, 128.5 (2 C), 126.0, 117.3 (2 C), 110.1, 109.7, 108.3, 95.3, 95.1, 94.5, 78.4, 77.9, 56.9, 56.5, 46.4, 39.2, 38.5, 29.0, 27.6, 20.1, 18.8, 14.8 ppm; $[\alpha]_{20}^{D}$ +70.8° (*c* 0.5 in CH_3CN); HRMS (ESI): *m/z* calcd. for $C_{29}H_{35}O_8^+$ $[M+H]^+$ 511.2326; found: 511.2326; IR: *v* 2927, 1635, 1602, 1510, 1434, 1343, 1240, 1152, 1079, 989, 836 cm^{-1}.

(7a*R*,9*R*,11a*R*)-6,9-dihydroxy-8,8,11a-trimethyl-3-phenyl-7a,8,9,10,11,11a-hexahydro-1*H*,7*H*-pyrano[2,3-*c*]xanthen-1-one (*R*,*R*,*R*)-12. A mixture of *(R,R,R)*-**10** (28 mg, 0.06 mmol) in CH_3CN (0.6 mL) was heated to 35 °C. A solution of HCl 2 M (0.62 mL, 20 eq) was added, and the mixture was stirred for 4 days at 35 °C. After cooling down, the reaction mixture was filtered to retain the expected crystallized product that was washed with cold CH_3CN and water. After drying, (*R*,*R*,*R*)-**12** (10 mg, 40%) was obtained as a yellow solid. ^{1}H NMR (500 MHz, DMSO-d_6): *δ* 10.7 (s, 1 H), 7.99-7.95 (m, 2 H), 7.57-7.51 (m, 3 H), 6.59 (s, 1 H), 6.55 (s, 1 H), 4.61 (d, J = 5.4 Hz, 1 H-OH), 3.27-3.22 (m, 1 H), 2.63 (dd, *J* = 17.3, 5.3 Hz, 1 H), 2.31 (dd, *J* = 17.3, 12.0 Hz, 1 H), 1.97-1.92 (m, 1 H), 1.75–1.68 (m, 2 H), 1.58–1.49 (m, 2 H), 1.14 (s, 3 H), 1.02 (s, 3 H), 0.79 (s, 3 H) ppm; ^{13}C NMR (125 MHz, DMSO-d_6): *δ* 175.4, 160.0, 159.0, 157.0, 153.7, 131.2, 131.1, 129.0 (2 C), 125.8 (2 C), 108.0, 107.2, 106.9, 93.8, 77.0, 75.9, 46.1, 38.0, 37.3, 28.0, 27.2, 19.5, 17.6, 14.4 ppm; $[\alpha]_{20}^{D}$ +44 ° (*c* 1 in MeOH); HRMS (ESI): *m/z* calculated for $C_{25}H_{27}O_5^+$ $[M + H]^+$: 407.1853; found: 407.1857; IR: *v* 3337, 2937, 1634, 1585, 1452, 1357, 1085, 1030 cm^{-1}.

(7a*S*,9*S*,11a*S*)-6,9-dihydroxy-8,8,11a-trimethyl-3-phenyl-7a,8,9,10,11,11a-hexahydro-1*H*,7*H*-pyrano[2,3-*c*]xanthen-1-one (*S*,*S*,*S*)-12. The same procedure starting from *(S,S,S)*-**10** that gave (*S*,*S*,*S*)-**12** (95%). $[\alpha]_{20}^{D}$ -54 ° (*c* 0.5 in MeOH).

(7a*R*,9*R*,11a*R*)-6,9-dihydroxy-3-(4-hydroxyphenyl)-8,8,11a-trimethyl-7a,8,9,10,11,11a-hexahydro-1*H*,7*H*-pyrano[2,3-*c*]xanthen-1-one (*R*,*R*,*R*)-13. Same procedure as for the synthesis of compound (*R*,*R*,*R*)-**12** using 40 eq of a solution of HCl 2 M. Compound **13** was obtained with 97% yield as a yellow solid. ^{1}H NMR (500 MHz, MeOD): *δ* 7.79 (d, *J* = 8.0 Hz, 2 H), 6.92 (d, *J* = 8.5 Hz, 2 H), 6.58–6.48 (m, 2 H), 3.39 (dd, *J* = 11.7, 4.2 Hz, 1 H), 2.78 (dd, *J* = 16.9, 5.0 Hz, 1 H), 2.43 (dd, *J* = 16.2, 14.0 Hz, 1 H), 2.24–2.16 (m, 1 H), 1.91–1.80 (m, 2 H), 1.73–1.58 (m, 2 H), 1.26 (s, 3 H), 1.12 (s, 3 H), 0.91 (s, 3 H) ppm; ^{13}C NMR (125 MHz, MeOD): *δ* 180.5, 163.4, 162.4, 162.2, 159.4, 155.5, 129.0 (2 C), 123.5, 117.0 (2 C), 109.1, 108.4, 106.6, 95.0, 79.3, 78.7, 47.1, 39.6, 38.5, 29.1, 27.9, 19.9, 19.1, 14.9 ppm; $[\alpha]_{20}^{D}$ +70.0° (*c* 0.5 in MeOH); HRMS (ESI): *m/z* calcd. for $C_{25}H_{27}O_6^+$ $[M+H]^+$ 423.1802; found: 423.1802; IR: *v* 3220, 2934, 1629, 1606, 1454, 1355, 1252, 1177, 1083, 1024, 836 cm^{-1}.

Protein expression and purification. The human OSBP ORD fragment (401-807) with a C-terminal 6×His tag was purified from baculovirus-infected Sf9 cells. For experimental details, see [21].

Liposomes. ER-like liposomes contain: egg PC/brain PS (95/5 mol%) and Golgi-like liposomes contain: egg PC/liver PE/brain PS/liver PI/DNS-PE (63.5/19/5/10/2.5 mol%). Egg PC (L-α-phosphatidylcholine), liver PI (L-α-phosphatidylinositol), liver PE (L-α-phosphatidylethanolamine), brain PS (L-α-phosphatidylserine), and DNS-PE (1,2-dioleoyl-*sn*-glycero-3-phosphoethanolamine-N-(5-dimethylamino-1-naphthalenesulfonyl)) were purchased from Avanti Polar Lipids. Dehydroergosterol (DHE) was from Sigma Aldrich. For the preparation of liposomes see [14].

Sterol transfer assay. The human OSBP ORD fragment (401-807) with a C-terminal 6×His tag was expressed and purified from baculovirus-infected Sf9 cells as previously described.[21] Golgi-like liposomes and ER-like liposomes supplemented with 18 mol% DHE were mixed in HKM buffer (HK buffer supplemented with 1 mM $MgCl_2$) in the presence of macarangin B analogues as in [14] (different stock concentration in DMSO, DMSO/buffer final ratio v/v 1/100), prior to the addition of OSBP ORD (100 nM final concentration). The sterol transport activity was monitored by FRET between DHE and DNS-PE, measured at 525/5 nm upon excitation at 310/1.5 nm in a Jasco FP-8300 spectrofluorimeter using a cylindrical quartz cuvette (600 µL) equilibrated at 37 °C and equipped with a magnetic bar for continuous stirring. Data analysis: Curves were fitted either with a linear equation (for slow kinetics) or, for fast kinetics, with an exponential equation $\Delta \boldsymbol{F} = \Delta \boldsymbol{F_{max}}(\mathbf{1} - \boldsymbol{e^{-kt}})$, to determine the apparent kinetic constant, k.[13] The apparent kinetic constant (k) obtained for each kinetic was then plotted against the concentration of the drugs. From this representation, we determined the inhibition constant Ki for each compound using either a quadratic (for potent inhibitors) or a hyperbolic equation (for weak inhibitor (*S*)-**10**).

Docking simulations. The 3D crystal structure of OSBP ORD was downloaded from the Protein Data Bank (PDB ID: 7v62[i]) and saved in pdb format. It was composed of four monomers complexed with cholesterol, citric acid, 2,3-dihydroxy-1,4-dithiobutane, DMSO and water. The file was first pre-processed with AutoDockTools. Three out of four monomers were discarded as well as water and complexed compounds. In the monomeric structure of chain A, missing atoms, polar hydrogen atoms and Gasteiger charges were added. The docking area was selected and the grid was saved as a txt file. Finally, the protein was split in two moieties (as pdbqt files), a flexible one containing 26 amino acids corresponding to those of the binding site (LEU16, MET20, LEU28, MET33, PHE37, MET43, ARG46, LEU47, ASP50, SER80, TYR81, THR84, ARG87, THR88, SER89, LYS90, PRO91, ILE142, LEU151, ILE153, PRO155, LYS174, THR177, VAL179, LEU187, ILE189) and a rigid one corresponding to the rest of the ORD domain. All the ligand were drawn on Avogadro, the energy of their 3D structure was minimized with ORCA, using Hartree–Fock method, and the STO-3G basis set. Xyz ligand files were then prepared in OpenBabel GUI, and saved as a pdbqt file. Ligands were docked within the flexible moiety of the protein (in the preconfigured grid box). The exhaustiveness was set to 20, the number of conformations generated for each ligand was set to 50, and the energy range to 4. Docking simulations were run with AutoDock Vina v1.1.2 on a Dell Precision 7760. The docked conformations of each compound were clustered based on their geometry and the clusters were ranked based on their binding energy. The ten most favorable binding conformations clusters, with the lowest free energies, were selected and visually analyzed. For each molecule, we determined the best docking pose by examining the lowest energy poses. A Python script (Result_Treatment.py) was developed in order to extract each model, and generate the protein with flexible residues included for each model. The protein-ligand 3D visualization was processed using PyMOL software. The 2D visualization of the interaction between the hybrids and the amino-acid residues of the ORD domain of OSBP was performed using BIOVIA Discovery Studio (Dassault System).

Cells, Virus and Reagents. Human lung epithelial A549 cells (ATCC, CCL-185) and Vero E6 cells (ATCC, CCL-81) were cultivated at 37 °C and 5% CO_2 in Dulbecco's Modified Eagle Medium (DMEM) containing 4.5 g/L of D-Glucose and supplemented with 10% FCS, 100 U/mL penicillin, 100 µg/mL streptomycin, 2 mM L-Glutamine, 0.5 µg/mL fungizone and 1 mM sodium pyruvate. ZIKV strain $MR766^{MC}$ used in this study has been previously described.[24] The ZIKV progeny production is determined by measuring the quantity of infectious virus particles released into the supernatant of infected cells by plaque-forming assay on Vero E6 cells.

Cell viability assay. A mitochondrial activity assay was performed to assess the toxicity of compounds in host cells prior to antiviral evaluation. A549 cells (2 x 10^4 cells/well) were seeded into 96-well plate and treated with two-fold dilutions of compounds ranging from 200 000 nM to 2 nM during 48 h or 72 h at 37 °C. Following treatment, the cells were washed, and 20 µL of MTS reagent mixed with 80 µL of culture medium was added to each well. The plates were incubated for 1 hour at 37 °C to allow the formation of formazan. Absorbance was then measured at 490 nm using a microplate reader. The CC_{50} values, representing the concentration at which 50% of cell viability is reduced, were determined by fitting the

data to a nonlinear regression model using GraphPad Prism software. Data are presented as mean ± SEM from three independent experiments.

Antiviral assay. A549 cells were infected with ZIKV at a multiplicity of infection (MOI) of 1 and simultaneously treated with various non-cytotoxic concentrations of compounds. At 24 h post-infection (pi), supernatants were collected and viral growth was quantified using a plaque forming assay. Briefly, Vero E6 cells were seeded in 24-well culture plates at a density of 8×10^4 cells per well and incubated overnight at 37 °C. Serial ten-fold dilutions of the supernatant were prepared in duplicate using culture medium, and 0.1 mL of each dilution was added to Vero E6 cells. After 2 hours of incubation, 0.2 mL of culture medium containing 5% fetal bovine serum (FBS) and 1 % carboxymethylcellulose sodium salt was added. The cells were further incubated for 4 days at 37 °C. Following incubation, the medium was carefully removed, and the cells were fixed with 3.7% paraformaldehyde (PFA) and stained with 0.5% crystal violet dissolved in 20% ethanol. Plaques was counted and the viral titer was expressed as plaque-forming units per milliliter (PFU/mL). Nonlinear regression was used to generate sigmoidal dose-response curves for determining inhibitory concentrations (IC_{50}). Data are presented as mean ± SEM from at least three independent experiments.

***In vitro* mouse plasma stability.** Experiments were performed at 37 °C in male mouse plasma supplied by Biopredic (France). Reactions were initiated by the addition of a 5 µM solution of test compounds 2, 12 or 15 to preheated plasma solution to yield a final concentration of 2.5 µM. Samples were collected at 0, 15, 30, 45, 60, and 120 min and acetonitrile was immediately added to stop the reaction. Samples were subjected to centrifugation for 10 min at 20,000 g at 4 °C and the clear supernatants were analyzed by LC-MS/MS with multiple reaction monitoring (MRM). All incubations were performed in duplicate. Procaine was used as the positive control. The MRM area response of the analyte for time = 0 (control) was set to 100%. The relative decrease in MRM area intensity over time against that of the control (percent parent decrease) was used to determine the half-life of elimination (t1/2) and the percentage of the remaining compound at 120 min. The UPLC−MS/MS system consisted of a Waters ACQUITY UPLC® System coupled to a Waters XEVO™ TQ-S Mass Spectrometer operating in positive ion electrospray MRM mode. All solvents and chemicals were of LC/MS grade and were purchased from VWR International.

Metabolic stability in mouse microsomes. Compounds **12**, **13** or **14** (2.5 µM) were incubated in NADPH (1 mM) and 0.1 M, pH 7.4 phosphate buffer at 37 °C. After pre-warming the mixture for 5 min, reactions were initiated by the addition of 0.5 mg/mL of pooled male mouse microsomes (Biopredic, France). Samples were collected at 0, 5, 15, 30, 45 min, and acetonitrile was immediately added to stop the reaction. Samples were centrifuged 10 min at 20,000 g at 4 °C and the supernatants were analyzed by LC-MS/MS with multiple reaction monitoring (MRM). All incubations were performed in duplicate. Diphenhydramine was used as the positive control. The MRM area response of the analyte for time = 0 (control) was set to 100%. The relative decrease in MRM area intensity over time against that of the control (percent parent decrease) was used to determine the half-life of elimination (t1/2) of compound in the incubation. Half-life values were calculated from the relationship: t (min) = 0.693/k, where k is the slope of the Ln concentration *vs.* time curve. The intrinsic clearance (Clint) was calculated as: Clint = (0.693 x incubation volume (µL))/(t (min) x mg of microsomal protein). Percentage of metabolism non-NADPH dependent was also monitored up to end-point incubation without NADPH.

Supporting Information

Supplementary figures, procedure for the synthesis of *rac*-**10**, and analytical data for all compounds.

Acknowledgements

We thank Dr Bruno Antonny for fruitful discussion. This work was supported by a maturation program grant managed by the SATT Paris-Saclay (CM2017-0045). G. J. was supported by a PhD fellowship from the Université Paris Saclay (ED ITFA). The study was supported by the French government as part of France 2030 with the support of ANRS I MIE through the ANRS-23-PEPR-MIE 0004 project intitled CAZIKANO. J. G. was supported by a PhD fellowship from INSERM in the framework of CAZIKANO project.

Keywords: Natural Product• Antiviral • OSBP • ADMET

[1] C. S. Adamson, K. Chibale, R. J. M. Goss, M. Jaspars, D. J. Newmane, R. A. Dorrington, *Chem.Soc. Rev.* **2021**, 50, 3647.

[2] WHO, W. H. O. A scientific framework for epidemic and pandemic research preparedness. **2024,** 12.

[3] G. Kuno in *Molecular Detection of Human Viral Pathogens* (Ed. : D. Liu), Routledge, Taylor& Francis Group, **2016**, *503*, pp.313-320.

[4] D. Barajas, K. Xu, I. F. de Castro Martín, Z. Sasvari, F. Brandizzi, C. Risco, P. D. Nagy, *PLoS Pathogens* **2014**, *10*, 34.

[5] F. Meutiawati, B. Bezemer, J. R P M Strating, G. J Overheul, E. Žusinaite, F. J. M. van Kuppeveld, K. W. R. van Cleef, R. P. van Rij, *Antiviral Research* **2018,***157*, 68.

[6] J. R. Strating, F. J. M. van Kuppeveld, *Curr Opin Cell Biol* **2017**, *47*, 24.

[7] B.L Roberts, Z. C. Severance, R. C. Bensen, A.T. Le-McClain, C. A. Malinky, E. M. Mettenbrink, J. I. Nuñez, W. J. Reddig, E. L. Blewett, A. W. G. Burgett, *Antiviral Research* **2019**, *170*, 104548.

[8] M. Arita, H. Kojima, T. Nagano, T. Okabe, T. Wakita, H. Shimizu, *J. Virol.* **2013**, *87*, 4252.

[9] B. L. Roberts, Z. C. Severance, R. C. Bensen, A. T. Le, N. R. Kothapalli, J. I. Nuñez, H. Ma, S. Wu, S. J. Standke, Z. Yang, W. J. Reddig, E. L. Blewett, A. W. G. Burgett, *ACS Chem. Biol.* **2019**, *14*, 276.

[10] J. R. P. M. Strating, L. van der Linden, L. Albulescu, J. Bigay, M. Arita, L. Delang, P. Leyssen, H. M. van der Schaar, K. H. W. Lanke, H. J. Thibaut, R. Ulferts, G. Drin, N. Schlinck, R. W. Wubbolts, N. Sever, S. A. Head, J. O. Liu, P. A. Beachy, M. A. De Matteis, M. D. Shair, V. M. Olkkonen, J. Neyts, F. J. M.van Kuppeveld, *Cell Reports* **2015**, *10*, 600.

[11] A. W. G.Burgett, T. B. Poulsen, K. Wangkanont, D. R. Anderson, C. Kikuchi, K. Shimada, S. Okubo, K. C. Fortner, Y. Mimaki, M. Kuroda, J. P. Murphy, D. J. Schwalb, E. C. Petrella, I. Cornella-Taracido, M. Schirle, J. A. Tallarico, M. D. Shair, *Nat Chem Biol* **2011**, *7* , 639.

[12] Y. D. Boyko, C. J.Huck, D. Sarlah, *J. Am. Chem. Soc.* **2019***, 141*, 14131.

[13] G. Jézéquel, C. Rampal, C. Guimard, D. Kovacs, J. Polidori, J. Bigay, J. Bignon, L. Askenatzis, M. Litaudon, V.-C. Pham, D. T. M. Huong, A. L. Nguyen, A. Pruvost, T. Virolle, B. Mesmin, S. Desrat, B. Antonny, F. Roussi, *J. Med. Chem.* **2023**, *66*, 14208.

[14] G. Jézéquel, Z. Grimanelli, C. Guimard, J. Bigay, J. Haddad, J. Bignon, C. Apel, V. Steinmetz, L. Askenatzis, H. Levaïque, C. Pradelli, V. C. Pham, D. T. M. Huong, M. Litaudon, R. Gautier, C. El Kalamouni, B. Antonny, S. Desrat, B. Mesmin, F. Roussi, *ChemRxiv preprint* **2024**, 10.26434/chemrxiv-2024-3b08x

[15] S. Ramešová, R. Sokolová, I. Degano, J. Bulíčková, J. Zabka, M. Gál, *Anal. Bioanal. Chem.* **2012**, *402*, 975.

[16] S. Maini, H. L. Hodgson, E. S. Krol, *J. Agric. Food Chem.* **2012**, *60*, 6966.

[17] J. Quintin, G. Lewin, *Tet. Lett.* **2004**, *45*, 3635.

[18] G. Dutheuil, N. Selander, K. Szabó, V. Aggarwal, *Synthesis* **2008**, 2293.

[19] B. Mesmin, J. Bigay, J. Moser von Filseck, S. Lacas-Gervais, G. Drin, B. A Antonny, *Cell* **2013**,*155*, 830.

[20] M. Subra, B. Antonny, B. Mesmin, *Curr Opin Cell Biol* **2023**, *82*, 102172.

[21] B. Mesmin, J. Bigay, J. Polidori, D. Jamecna, S. Lacas-Gervais, B. Antonny, *Embo J* **2017**, *36*, 3156.

[22] T. Péresse, D. Kovacs, M. Subra, J. Bigay, M.-C. Tsai, J. Polidori, R. Gautier, S. Desrat, L. Fleuriot, D. Debayle, M. Litaudon, V.-C. Pham, J. Bignon, B. Antonny, F. Roussi, B. Mesmin, *J Biol Chem* **2020**, *295*, 4277.

[23] J. Kobayashi, M. Arita, S. Sakai, H. Kojima, M. Senda, T. Senda, K. Hanada, R. Kato, *ACS Infect. Dis.*, **2022**, *8,* 1161.

[24] G. Gadea, S. Bos, P. Krejbich-Trotot, E. Clain, W. Viranaicken, C. El-Kalamouni, P. Mavingui, P. Desprès, *Virology* **2016**, *497*, 157.